Auris Nasus Larynx xxx (2017) xxx–xxx

Contents lists available at ScienceDirect

Auris Nasus Larynx

journal homepage: www.elsevier.com/locate/anl

A high jugular bulb and poor development of perivestibular aqueductal air cells are not the cause of endolymphatic hydrops in patients with Ménière's disease

Ryohei Oya [a], Takao Imai [a,*], Takashi Sato [a], Atsuhiko Uno [b], Yoshiyuki Watanabe [c], Suzuyo Okazaki [d], Yumi Ohta [a], Tadashi Kitahara [e], Arata Horii [f], Hidenori Inohara [a]

[a] *Department of Otorhinolaryngology — Head and Neck Surgery, Osaka University Graduate School of Medicine, Osaka, Japan*
[b] *Department of Otorhinolaryngology — Head and Neck Surgery, Osaka General Medical Center, Osaka, Japan*
[c] *Department of Diagnostic and Interventional Radiology, Osaka University Graduate School of Medicine, Osaka, Japan*
[d] *Department of Otolaryngology, Osaka City General Hospital, Japan*
[e] *Department of Otorhinolaryngology — Head and Neck Surgery, Nara Medical University, Nara, Japan*
[f] *Department of Otorhinolaryngology — Head and Neck Surgery, Niigata University Graduate School of Medicine and Dentistry, Niigata, Japan*

ARTICLE INFO

Article history:
Received 17 June 2017
Accepted 14 September 2017
Available online xxx

Keywords:
Ménière's disease
Endolymphatic hydrops
Gadolinium-enhanced magnetic resonance imaging
High jugular bulb
Computed tomography

ABSTRACT

Objective: The presence of endolymphatic hydrops in the inner ear, which can be detected with gadolinium-enhanced magnetic resonance imaging (Gd-MRI), is widely recognized as the main pathological cause of Ménière's disease (MD). However, the precise mechanisms underlying the development of endolymphatic hydrops remains unclear. One hypothesis proposes a relationship between the presence of a high jugular bulb (HJB) and MD, which disrupts the vestibular aqueduct leading to the development of endolymphatic hydrops. This study sought to identify anatomical features in MD patients using computed tomography (CT) images of the temporal bone.
Methods: Fifty-nine MD patients meeting the AAO-HNS diagnostic criteria and exhibiting endolymphatic hydrops in Gd-MRI were enrolled between July 2009 and December 2015. We only included MD patients who showed unilateral endolymphatic hydrops in Gd-MRI. Sixty-six patients with otosclerosis or facial palsy were also enrolled as control participants. In both groups, patients with other pathologies (e.g., chronic otitis media or cholesteatoma) and patients <16 years old were excluded. HJB was defined as a JB that was observable in the axial CT image at the level where the round window could be visualized. JB surface area was measured on the axial image at the level where the foramen spinosum could be visualized. Finally, to investigate the relationship between the pneumatization of perivestibular aqueductal air cells and the existence of endolymphatic hydrops, the development of the air cells was rated using a three-grade evaluation system and the distance between the posterior semicircular canal (PSCC) and the posterior fossa dura was measured.
Results: The presence of HJB was observed in 22 of 59 affected sides of MD patients and in 17 healthy sides. The likelihood that HJB was detected on an affected side (22/39) was not significantly above chance (50%). The HJB detection rate did not significantly differ between the three groups (MD affected side, MD healthy side, and control patients). Furthermore, there were no significant group differences in JB surface area, distance between the PSCC and posterior fossa dura, or the development of perivestibular aqueductal air cells.

* Corresponding author at: Department of Otorhinolaryngology — Head and Neck Surgery, Osaka University Graduate School of Medicine, 2-2 Yamadaoka, Suita-shi, Osaka 565-0871, Japan. Fax: +81 6 6879 3959.
E-mail address: timai@ent.med.osaka-u.ac.jp (T. Imai).

http://dx.doi.org/10.1016/j.anl.2017.09.014

Conclusion: We did not find any relationship between the anatomy of the temporal bones and the existence of endolymphatic hydrops. Moreover, we found no evidence suggesting that HJB or poor development of perivestibular aqueductal air cells were the cause of endolymphatic hydrops in MD patients.

1. Introduction

The presence of endolymphatic hydrops in the inner ear is widely recognized as a pathological cause of Ménière's disease (MD), as suggested by histopathological examinations of the temporal bone [1]. According to the diagnosis guidelines for MD, a true diagnosis requires the identification of vestibular and cochlear hydrops by cadaveric investigation [2]. However, confirmation via cadaveric investigation is not performed in most cases of MD diagnosis. Therefore, several attempts have been made to identify in vivo biomarkers of endolymphatic hydrops in the inner ear. These include the use of an electrocochleogram (EcochG) to obtain the dominant negative summating potential/action potential ratio (−SP/AP), the evaluation of the hearing improvement level using the glycerol test, and the measure of the vestibulo-ocular reflex (VOR) gain increase after the administration furosemide (i.e., furosemide test) [3]. Furthermore, it was recently reported that hydrops can also be detected by inner ear magnetic resonance imaging (MRI) following the intratympanic or intravenous administration of gadolinium (Gd-MRI) [4–6]. Current evidence suggests that Gd-MRI, compared with alternative methods, has the highest efficacy rate (about 90%) for the detection of endolymphatic hydrops [7]. Gd-MRI allows for the visualization of an enlarged endolymphatic space, which appears as low-intensity signal areas in MD patients. Although endolymphatic hydrops can be observed in MD patients, the precise causes of the phenomenon remain unclear and controversial.

MD typically develops unilaterally (i.e., in a single ear) suggesting that specific lateralized anatomical factors may trigger the emergence of hydrops. Indeed, several reports have suggested that the anatomy surrounding the temporal bone in MD patients plays a specific role. For instance, the morphology of the dural venous sinuses, such as the presence of a high jugular bulb (HJB) or a jugular bulb (JB) diverticulum, is highly variable across individuals. The anatomy of the dural venous sinuses is shaped by both the embryologic and postnatal development of the brain and by lifelong cerebral circulation. Anatomical abnormalities of the dural venous sinuses can extend into the middle and inner ear, and are associated with a variety of symptoms, including tonal or pulsatile tinnitus, vertigo, and hearing loss [8]. Wadin et al. reported that HJBs could be reliably identified with a high probability in MD patients using computed tomography (CT) to image the temporal bone [9] and suggested that HJB might induce hydrops by disturbing the vestibular aqueduct. Furthermore, Jarhrsdoerfer et al. surgically demonstrated that HJB could obstruct the vestibular aqueduct [10]. Other studies have previously reported poor development of perivestibular aqueductal air cells in MD patients, possibly caused by the presence of HJB [11–13].

The present study sought to identify anatomical features of the temporal bone that potentially underlie the emergence of endolymphatic hydrops in MD patients, by analyzing the CT images of MD patients in whom Gd-MRI had previously revealed unilateral endolymphatic hydrops.

2. Materials and methods

Patients diagnosed with unilateral definite MD (AAO-HNS) [2] participated in this study. All participants developed unilateral hearing impairment and had frequent episodes of definitive vertigo spells (at least once a month for the past 6 months on average, with a maximal interval of 2 months between episodes), as defined by the AAO-HNS diagnostic criteria [2]. All MD patients also exhibited endolymphatic hydrops in the inner ear, as evidenced by Gd-MRI scans obtained between July 2009 and December 2015 [5,6]. Patients with otosclerosis or facial palsy (without a diagnosis of MD) also participated in the present study as control participants. For both groups, cases with poor pneumatization in the mastoid cavity due to chronic otitis media, with cholesteatoma or other pathologies, and patients <16 years old were excluded from the present study. Furthermore, a single bilateral MD case and any MD patients who did not show endolymphatic hydrops in enhanced MRI were also excluded. This resulted in a final sample of 59 patients with MD (28 men, 31 women; median age 60 years; age range 33–79 years) and 66 control patients (132 ears) with either otosclerosis or facial palsy (33 men, 33 women; median age 44.5 years; age range 17–82 years). The present study was approved by the ethics committee at our hospital and was performed in accordance with the Declaration of Helsinki. Written informed consent was obtained from all patients.

2.1. Gd-MRI

We used two types of gadolinium (Gd) administration: intratympanic and intravenous. The intratympanic method used Gadodiamide hydrate (Omniscan®) diluted eightfold in saline, injected into the affected tympanic cavity; MRI images were acquired 24 h after the injection [5]. The intravenous method used a double dose of gadoteridol (Prohance® 0.4 ml/kg), injected intravenously; MRI images were acquired 4 h after injection [6,14]. The intratympanic method was performed for three patients, and the intravenous method was performed for 56 patients. All MR images were obtained with a 3 T MRI unit (Sigma Excite HD 3T, GE Healthcare) using a two-dimensional fluid attenuated inversion recovery (2D-FLAIR) acquisition sequence for hydrops evaluation. 2 mm thick axial images were adjusted parallel to the anterior commissure-posterior commissure line in an identical manner to the standard routine for MR

Please cite this article in press as: Oya R, et al. A high jugular bulb and poor development of perivestibular aqueductal air cells are not the cause of endolymphatic hydrops in patients with Ménière's disease. Auris Nasus Larynx (2017), http://dx.doi.org/10.1016/j.anl.2017.09.014

images. In the inner ear, only the perilymphatic space was contrast-enhanced by the Gd agent, whereas the endolymphatic space was visible as a low signal intensity area [4,5]. To detect hydrops, we compared the 2D-FLAIR images with constructive interference in steady-state (CISS) images of the same slice. Our criteria for identifying inner ear hydrops in Gd-enhanced MR images were based on the method outlined by Uno et al. [6]. We categorized each image as either "positive (abnormal)" or "negative (normal)" regarding the presence of endolymphatic hydrops. Images were qualitatively judged to be positive when the low-intensity signal areas corresponding to the cochlear duct could be clearly observed. These low-intensity signal areas should be at the edges of the cochlea and should be easily distinguishable from the bony structures surrounding it. The images were positive for vestibular hydrops when more than 33.3% of the vestibule was occupied by a low signal area [6,14].

Fig. 1 shows the 2D-FLAIR images of the affected right ear from MD patient 1 (a 46-year old woman). Fig. 1A shows the original 2D-FLAIR images. Comparing these 2D-FLAIR images with CISS images of the same slice, we manually traced the outline of the perilymphatic space and the cochlea using a white line. The enclosed vestibule is shown in white, whereas the endolymphatic space of the vestibule and the cochlea are shown in black, as seen in Fig. 1B. As illustrated by the black triangles in Fig. 1B, the black areas were located at the edge of the cochlea. Therefore, this image was judged to be positive for cochlear endolymphatic hydrops. Using the images shown in Fig. 1B, we calculated the volume of the vestibule and the endolymphatic space of the vestibule. The volume of the vestibule was 55.1 mm^3, the volume of the endolymphatic space of the vestibule was 26.2 mm^3, and the ratio of both volumes was 47.5% (26.2 mm^3/55.1 mm^3). Since the ratio was more than 33.3%, the image was judged to be positive for vestibule endolymphatic hydrops. Therefore, the images of MD patient 1 were judged to be positive for both cochlear and vestibular endolymphatic hydrops. In the present study, to evaluate inner ear hydrops, two of the authors (A.U. and/or A.H. and/or T.K.) independently examined Gd-MRI images prepared by others (T.I.) without any patient/group information.

2.2. CT scanning

CT imaging was performed on a 64-detector CT system (Discovery CT 750HD, GE healthcare, Milwaukee, USA) using a bone reconstruction algorithm and the following standard temporal bone protocol parameters: 120 kV, 250 mA, 0.531 pitch, 0.5 s rotation time, 0.6 mm slice thickness, 0.6 mm collimation, 512 × 512 matrix size, and field of view (FOV) of 12 cm aimed at the temporal bone. All images were displayed with a standardized window/level setting of 3000/300 HU using a DICOM workstation viewer. Measurements were obtained using electronic calipers and recorded in units of one-tenth of a millimeter. All measurements and morphological evaluations were performed by two otoneurologists (R.O. and T.S.). The images were first prepared by another author (T.I.). All measurements were performed blind with respect to the group assignment of each image.

Previous reports have operationally defined HJBs. For instance, a JB has been classified as HJB when: (1) it rises to the level of the basal turn of the cochlea [9], (2) the dome of the bulb encroaches within 2 mm of the floor of the internal auditory canal [15], (3) the bulb extends above the inferior tympanic annulus [16], and (4) the bulb rises above the round window [8,17]. We believe that the fourth definition is the most robust and reliable. Therefore, in the present study, HJB was defined as an instance in which the JB could be seen in the axial CT image above where the round window could be visualized. Fig. 2A shows an axial CT image of patient 1's right side at the level of the round window (indicated by a black star). In this image, a JB could be visualized. Therefore, it was concluded that HJB was present in the patient's right ear. In Fig. 2B, an axial CT image of patient 1's left ear is shown at the same level of Fig. 2A. In this image, the JB could not be seen. Therefore, it was concluded that there was no HJB in the left ear. In a similar manner, HJB screening was performed for both ears in all patients. The presence of HJB was compared between groups (MD affected side, MD healthy side, and control patients) using a Pearson's chi-square test. The level of statistical significance was set at $p = 0.05$. The surface area where a JB could be visualized on the same axial CT image as the foramen spinosum was also measured, following the method outlined by Friedman et al. [8]. In Fig. 2C, an axial CT image of patient 1's right ear is shown at the level where the foramen spinosum (indicated by a black arrow) could be visualized. We measured the JB surface area in the image (colored in black). The measured area for patient 1 was 91.9 mm^2. In a similar manner, the JB surface area was measured for both ears in all patients.

The development of pneumatization in the perivestibular aqueduct was rated with a three-grade evaluation: good, normal, or poor. A good rating was given when more air cells existed inside than in the vestibular aqueduct, whereas a poor rating was given when there were no air cells between the PSCC and the posterior fossa dura. A normal rating was given for cases falling between those constituting poor and good ratings. In Fig. 3A, an axial CT image of patient 1's right side is shown at the level at which the outermost side of the PSCC could be visualized. The pneumatization of perivestibular aqueductal air cells was judged to be normal in this image. Fig. 3B and C shows cases in which pneumatization was judged to be good (because more air cells were found inside than in the vestibular aqueduct, indicated by a thin black arrow) and poor (because there were no air cells between the PSCC and the posterior fossa dura), respectively. Specifically, Fig. 3B shows good pneumatization observed in an axial CT image of MD patient 2's right affected side (46 years old, female) at the level where the outermost side of the PSCC could be visualized, whereas Fig. 3C illustrates an axial CT image of MD patient 3's right affected side (73 years old, female) at the level where the outermost side of the PSCC could be visualized. The grade proportions were compared between groups using a Pearson's chi-square test. The level of statistical significance was set at $p = 0.05$.

To evaluate the development of the perivestibular aqueductal air cells quantitatively, the distance between the posterior semicircular canal (PSCC) and the posterior fossa dura was measured on the axial image where the outermost side of the

Please cite this article in press as: Oya R, et al. A high jugular bulb and poor development of perivestibular aqueductal air cells are not the cause of endolymphatic hydrops in patients with Ménière's disease. Auris Nasus Larynx (2017), http://dx.doi.org/10.1016/j.anl.2017.09.014

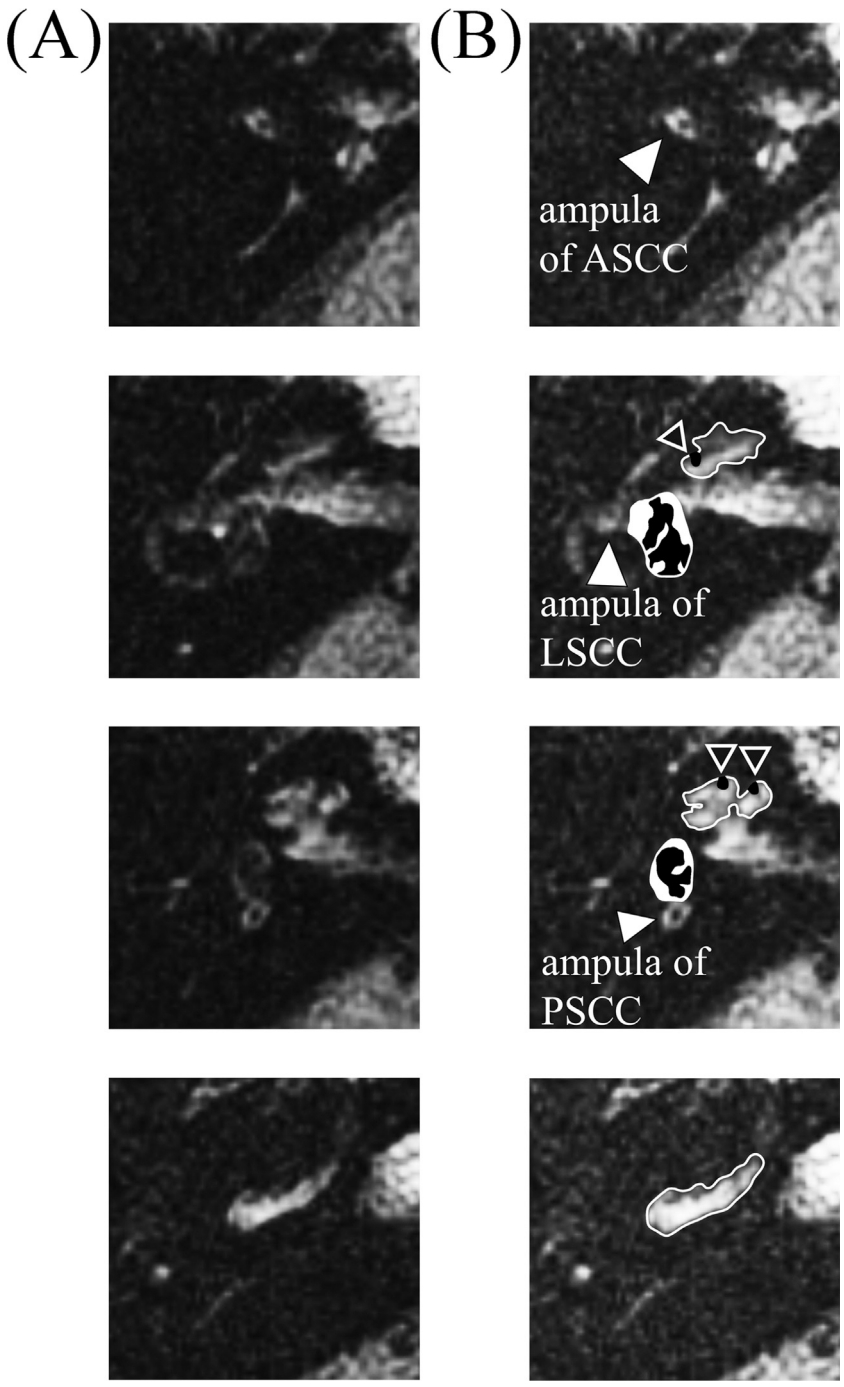

Fig. 1. Gadolinium-enhanced magnetic resonance imaging (Gd-MRI) of patient 1, who was affected on the right side.
(A) Original two-dimensional fluid-attenuated inversion recovery (2D-FLAIR) images of the right ear (axial view).
(B) Perilymphatic and endolymphatic spaces were manually drawn after comparing the 2D-FLAIR image and the constructive interference in a steady-state (CISS) image of the same slice level.
White areas indicate the perilymphatic space of the vestibule. Black areas indicate the endolymphatic space of the vestibule and the cochlea. Cochlear hydrops were located at the edge of the cochlea and are indicated by black triangles. ASCC: anterior semicircular canal, LSCC: lateral semicircular canal, PSCC: posterior semicircular canal.

PSCC could be observed. For example, as shown in Fig. 3A the distance between the PSCC (indicated by a thick white arrow) and the posterior fossa dura (indicated by a thick black arrow) was 2.8 mm. As shown in Fig. 3C, the distance was 0 mm, because no air cells were found between the PSCC and the posterior fossa dura. The surface area of JB and the distance between air cells were compared between groups (MD affected side, MD healthy side, and control patients) using one-way repeated measures analyses of variance. The level of statistical significance was set at $p = 0.05$. The choice of this significance level implies that a significant difference was present only when the test statistic F(2,247) was greater than 3.032.

Please cite this article in press as: Oya R, et al. A high jugular bulb and poor development of perivestibular aqueductal air cells are not the cause of endolymphatic hydrops in patients with Ménière's disease. Auris Nasus Larynx (2017), http://dx.doi.org/10.1016/j.anl.2017.09.014

Fig. 2. Axial CT images of patient 1.
(A) Axial CT image of the right side at the level where the round window could be observed.
A black star indicates the round window. Because the jugular bulb (JB) could be detected in this image, the patient's right side was judged to contain a high JB (HJB).
(B) Axial CT image of the left side at the same level as shown in (A). Because no JB could be detected in this image, it was concluded that no HJB was present on the patient's left side.
(C) Axial CT image of the right side at the level where the foramen spinosum could be observed.
The foramen spinosum is indicated by a black arrow. Using the image at this level, the JB surface area was measured. The black overlay represents a JB area equal to 91.9 mm^2.

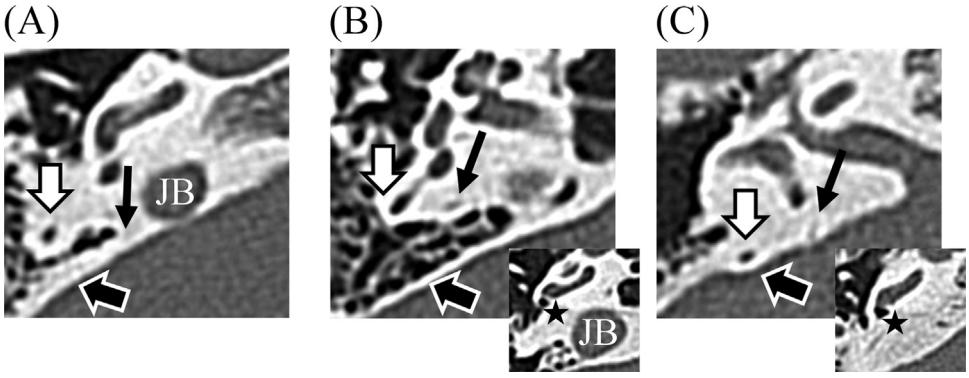

Fig. 3. Evaluation of the pneumatization of perivestibular aqueductal air cells.
(A) Normal pneumatization: This figure shows an axial CT image of patient 1's right side at the level where the outermost side of the PSCC could be observed. The pneumatization was judged to be normal because the air cells could be seen between the PSCC and the posterior fossa dura but no air cells could be seen inside the vestibular aqueduct (indicated by a thin black arrow). The distance between the PSCC (indicated by a thick white arrow) and the posterior fossa dura (indicated by a thick black arrow) was 2.8 mm.
(B) Good pneumatization: This figure shows an axial CT image of patient 2's right side at the level where the outermost side of the PSCC could be observed. The pneumatization was judged to be good because the air cells could be seen more inside than in the vestibular aqueduct. The distance between the PSCC and the posterior fossa dura was 5.0 mm. The inserted axial CT image is one of patient 2's right side at the level where the round window (indicated by a black star) could be observed.
(C) Poor pneumatization: This figure shows a CT image of patient 3's right side at the level where the outermost side of the PSCC could be observed. The pneumatization was judged to be poor because no air cells could be seen between the PSCC and the posterior fossa dura and the measured distance between both structures was 0 mm. The inserted axial CT image is that of patient 3's right side at the level where the round window could be observed.

3. Results

The images of Gd-MRI of all 59 MD patients were judged to be positive for either vestibular hydrops or cochlear hydrops. Twenty-six MD patients received a right-sided hydrops diagnosis, whereas the remaining 33 MD patients were diagnosed with hydrops in the left ear.

As shown in Table 1, the presence of HJB was not only observed in 22 out of the 59 affected sides in MD patients, but also in 17 non-affected sides. Therefore, HJB was observed in a total of 39 (22 + 17) sides, and only 56% of HJBs were localized on the affected side, a ratio that was not significantly above chance ($p = 0.261$). HJB was observed in 48 of a possible 132 sides in the control group. The HJB detection rate did not

Table 1
Group comparison of the side distribution of high jugular bulbs (HJB) and endolymphatic hydrops.

	Affected sides in MD patient	Healthy sides in MD patient	Control patients
HJB (+)	22	17	48
HJB (−)	37	42	84

There were no significant group difference regarding the likelihood of an HJB and endolymphatic hydrops occurring on the same side.

Please cite this article in press as: Oya R, et al. A high jugular bulb and poor development of perivestibular aqueductal air cells are not the cause of endolymphatic hydrops in patients with Ménière's disease. Auris Nasus Larynx (2017), http://dx.doi.org/10.1016/j.anl.2017.09.014

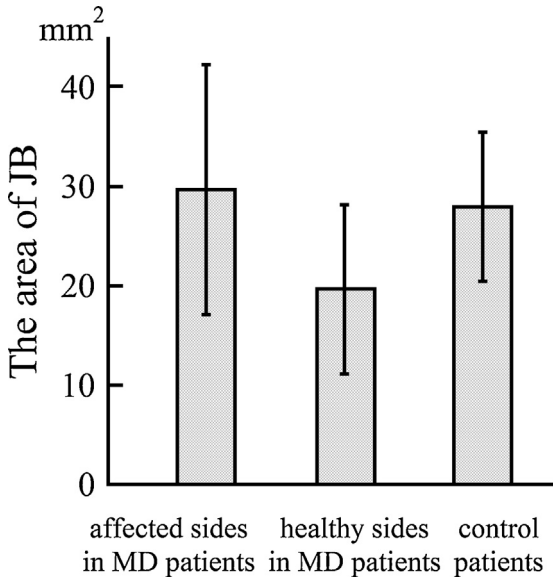

Fig. 4. The jugular bulb (JB) surface area.
Error bars show the 95% confidence interval. There were no statistically significant group differences.

statistically differ between the three groups (MD affected side, MD healthy side, and control patients) ($p = 0.5393$).

The average JB surface areas were 29.7 ± 49.3 mm^2 (mean $\pm$ standard deviation) and 19.6 ± 33.4 mm^2 for the affected and healthy sides of MD patients, respectively. The JB surface area for the control group was 28.0 ± 44.0 mm^2 (Fig. 4). There were no statistically significant group differences ($F(2,247) = 0.9855$, $p = 0.3747$).

Using the procedure described above, the pneumatization of perivestibular aqueductal air cells was assessed on both sides of all patients, and the associated grades are shown in Table 2. There were no statistically significant group differences ($p = 0.8039$).

Table 2
The evaluation of the pneumatization of perivestibular aqueductal air cells.

	Affected sides in MD patient	Healthy sides in MD patient	Control patients
Good	13	16	39
Normal	19	15	34
Poor	27	28	59

There were no statistically significant group differences with regards to the grade (good, normal, or poor) attributed to the pneumatization of perivestibular aqueductal air cells.

Fig. 5A shows the distance between the PSCC and the posterior fossa dura in both groups. The average distance was 1.4 ± 1.6 mm (mean $\pm$ standard deviation) on the affected side of MD patients, 1.3 ± 1.5 mm on the healthy side of MD patients, and 1.4 ± 1.6 mm in control patients. There were no statistically significant group differences ($F(2,247) = 0.0586$, $p = 0.9431$). Fig. 5B illustrates the relationship across individuals between the JB surface area and the distance between the PSCC and the posterior fossa dura for all three groups. The coefficient of determination (R^2) of the relationship was 0.0018 for the affected side of MD patients, 0.0002 for the healthy side of MD patients, and 0.0025 for control patients. In all cases, the correlation between the JB surface area and the distance between the PSCC and the posterior fossa dura was not statistically significant.

4. Discussion

Previous pathological examinations have found endolymphatic hydrops in the temporal bones of MD patients, and it has therefore been hypothesized that these hydrops potentially underlie the emergence of MD [1]. Recent developments in neuroimaging technology allow the detection of inner ear hydrops with Gd-enhanced MRI [4,5], aiding in the diagnosis of

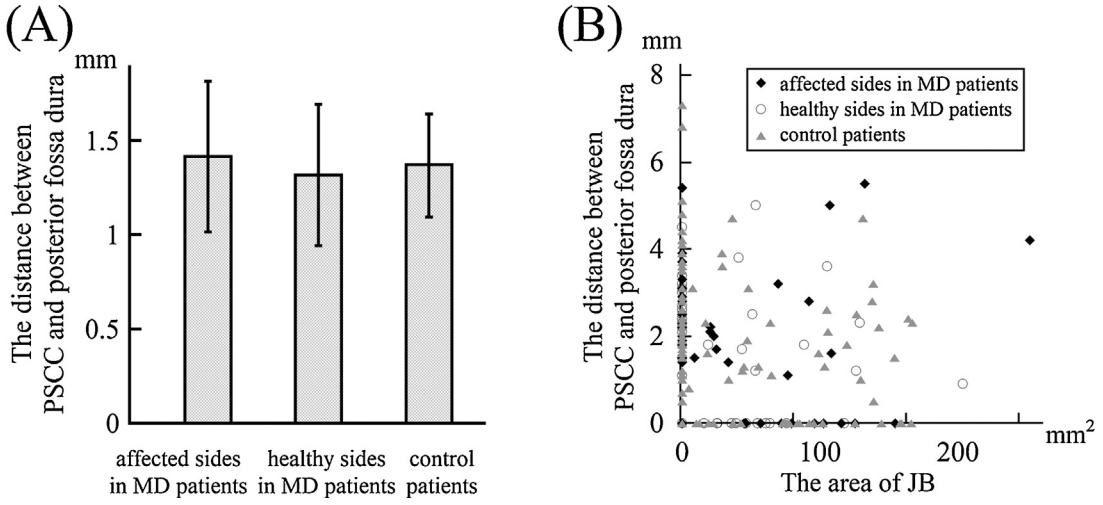

Fig. 5. The distance between the PSCC and the posterior fossa dura.
(A) This figure shows the distance between the PSCC and the posterior fossa dura.
Error bars show the 95% confidence interval. There were no statistically significant group differences.
(B) This figure shows the relationship between the area of JB and the distance between the PSCC and the posterior fossa dura via individual scatter plots for each group.
For all groups, the R^2 value of was near zero, strongly suggesting an absence of a relationship between the JB surface area and the distance between the PSCC and the posterior fossa dura.

Please cite this article in press as: Oya R, et al. A high jugular bulb and poor development of perivestibular aqueductal air cells are not the cause of endolymphatic hydrops in patients with Ménière's disease. Auris Nasus Larynx (2017), http://dx.doi.org/10.1016/j.anl.2017.09.014

MD. However, it remains unclear how hydrops develop and why they typically affect only one ear. This unilateral effect is believed to result from structural and anatomical differences between the right and left sides. Several previous reports have suggested a potential relationship between HJB and MD [9,10,18]. This proposed relationship is based on the hypothesis that HJB disturbs the vestibular aqueduct to the point of producing hydrops. However, in most of these reports, MD was only diagnosed using clinical symptoms, including those highlighted by the AAO-HNS guidelines, and did not confirm the existence of endolymphatic hydrops. In the present study, however, the existence of endolymphatic hydrops was confirmed by Gd-MRI and patients with bilateral endolymphatic hydrops were excluded. Therefore, we investigated the relationship between the presence of endolymphatic hydrops and structural temporal bone asymmetries using only MD patients who had unilateral endolymphatic hydrops. When MD patients had unilateral HJB, the likelihood of finding endolymphatic hydrops on the same side was not significantly above chance. Furthermore, there were no significant group differences regarding the likelihood of HJB and hydrops occurring on the same side (Table 1). Also, there were no group differences regarding the size of JBs (Fig. 4). Taken together, these results suggest that there is no relationship between the presence of HJB and the development of endolymphatic hydrops. These results further suggest that an obstruction of the vestibular aqueduct by HJB does not cause endolymphatic hydrops. In CT images in several cases, the JB was found to touch or penetrate the vestibular aqueduct. This finding may have reflected true obstruction of the vestibular aqueduct by HJB. However, there are no defined criteria for determining JB touching (penetration) of the vestibular aqueduct, and the judgment was subjective. Therefore, we did not analyze these findings in the present study.

An alternative hypothesis suggests that temporal bone anatomy influences the development of endolymphatic hydrops in the inner ear [8,9]. Specifically, it has been proposed that poor pneumatization of the perivestibular aqueductal air cells reduces the size of the endolymphatic sac, resulting in the development of endolymphatic hydrops [12]. In the present study, we investigated the pneumatization of perivestibular aqueductal air cells on both the affected and healthy sides of MD patients, as well as on both sides of control patients. The quality of pneumatization was not found to be significantly different between groups. Furthermore, we also investigated the distance between the PSCC and the posterior fossa dura, revealing no significant group differences. Although a previous report by Kennedy et al. hinted at a relationship between poor pneumatization of perivestibular aqueductal air cells and the development of HJB [13], our results, in contrast, suggest that there is no relationship between the existence of endolymphatic hydrops and poor pneumatization of perivestibular aqueductal

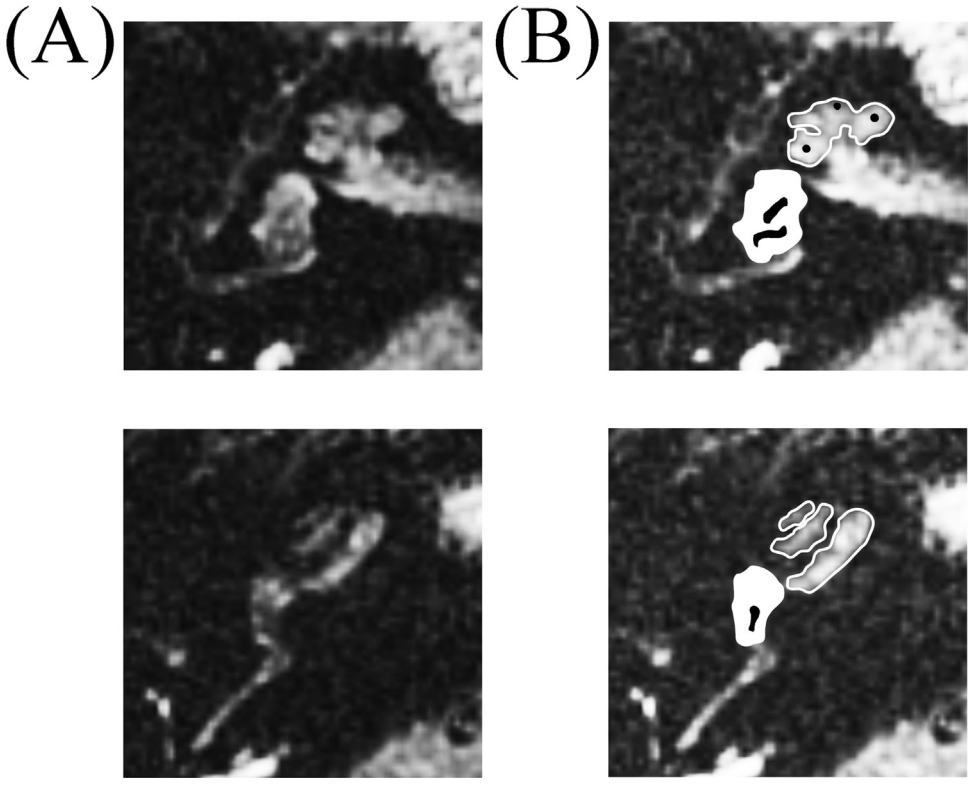

Fig. 6. Gd-MRI scan of patient 1 after a right side endolymphatic sac surgery.
(A) Original 2D-FLAIR images of the right ear (axial view).
(B) Perilymphatic and endolymphatic spaces were manually drawn after comparing the 2D-FLAIR image and the constructive interference in a steady-state image (CISS) of the same slice level.
White areas indicate the perilymphatic space of the vestibule. Black areas indicate the endolymphatic space of the vestibule and the cochlea. Cochlear hydrops were not found at the edge of the cochlea, suggesting that they had disappeared after surgery. Moreover, the ratio of endolymphatic space volume to vestibule volume was reduced to less than 33.3% following surgery, further suggesting the surgery contributed to removing the vestibular hydrops.

Please cite this article in press as: Oya R, et al. A high jugular bulb and poor development of perivestibular aqueductal air cells are not the cause of endolymphatic hydrops in patients with Ménière's disease. Auris Nasus Larynx (2017), http://dx.doi.org/10.1016/j.anl.2017.09.014

air cells. Furthermore, there was no correlation between JB surface area and the distance between the PSCC and the posterior fossa dura in any group (Fig. 5B). Indeed, as shown in Fig. 3A and B, the pneumatization of perivestibular aqueductal air cells on the right side of patients 1 and 2 were not found to be poor, even though HJB was present (Figs. 2 A and 3 B). In contrast, the pneumatization of perivestibular aqueductal air cells on the right side of patient 3 was found to be poor (Fig. 3C) despite the absence of HJB (Fig. 3C).

We performed endolymphatic sac surgery on the right side of patient 1. The result of the Gd-MRI scan after surgery is shown in Fig. 6. It can be seen that the endolymphatic space of the right cochlea was not at the edge of the cochlea, as it was before surgery (Fig. 1). Furthermore, although the size of the right vestibule was unchanged after surgery (55.1 mm^3 before surgery vs. 51.4 mm^3 after surgery), the size of the endolymphatic space of the right vestibule decreased dramatically after surgery (26.2 mm^3 before surgery vs. 4.1 mm^3 after surgery). The ratio of endolymphatic space volume to vestibule volume decreased below 33.3% (from 47.5% before surgery to 8.0% after surgery), suggesting that the placement of a shunt between the endolymphatic sac and the mastoid decreased the amount of pressure in the endolymphatic space. If obstruction of the vestibular aqueduct by HJB was indeed the cause of endolymphatic hydrops, the placement of a shunt would be an ineffective means of decreasing the amount of pressure in the endolymphatic space, because the endolymphatic sac sits more peripherally relative to the vestibular aqueduct. In our previous study, we reported that endolymphatic hydrops of four of seven cases was significantly reduced in postoperative enhanced MRI following a sac operation [6]. Overall, these findings further support our conclusion that the presence of HJB is likely not the cause of endolymphatic hydrops.

The present study involved several limitations that should be considered. First, the severity of MD, including the duration or stage, may have affected the results. However, in the present study we confirmed that all MD patients were suffering from vertigo attacks at least once a month for 6 months. Furthermore, the criteria for diagnosing endolymphatic hydrops in the present study were established by a group at Nagoya University [4], and are widely recognized as the standard method. Thus, in the present study, the disease duration and stage of MD patients was relatively severe. Therefore, it is less likely that the severity of MD and endolymphatic hydrops substantially affected the present results. Second, we measured the JB surface area on axial CT images, in reference to a previous report [8]. This measurement may reflect a tendency in the development of the JB. However, we could not confirm that the surface area definitely reflects HJB.

The current results indicated that neither the presence of HJB nor the poor pneumatization of perivestibular aqueductal air cells are significantly associated with endolymphatic hydrops. We also showed that unilateral incidence of endolymphatic hydrops was not caused by anatomical differences between the right and left temporal bones. This finding suggests that the underlying cause may be linked to other macro anatomical factors or micro anatomical factors such as a molecular or biochemical differences between both inner ears [19,20].

Funding

None.

Ethical approval

All procedures performed in studies involving human participants were in accordance with the ethical standards of the institutional research committee and with the 1964 Helsinki declaration and its later amendments or comparable ethical standards.

Informed consent

Informed consent was obtained from all individual participants included in the study.

Acknowledgments

This work was supported by JSPS KAKENHI Grant (Nos. 16H06957, 17K11327) and a Grant-in-Aid from the Japan Agency for Medical Research and Development. The ethics committee of Osaka University Hospital approved the study (Nos. 08223, 11341, 16329).

We thank Benjamin Knight, MSc, from Edanz Group (www.edanzediting.com/ac) for editing a draft of this manuscript.

References

[1] Paparella MM, Morizono T, Matsunaga T. Kyoshiro Yamakawa, MD, and temporal bone histopathology of Meniere's patient reported in 1938. Commemoration of the centennial of his birth. Arch Otolaryngol Head Neck Surg 1992;118:660–2.
[2] Committee on Hearing and Equilibrium. Guideline for the diagnosis and evaluation of therapy in Meniere's disease. Otolaryngol Head Neck Surg 1995;113:181–5.
[3] Ito M, Watanabe Y, Shojaku H, Kobayashi H, Aso S, Mizukoshi K. Furosemide VOR test for the detection of endolymphatic hydrops. Acta Otolaryngol 1993;113:55–7.
[4] Nakashima T, Naganawa S, Sugiura M, Teranishi M, Sone M, Hayashi H, et al. Visualization of endolymphatic hydrops in patients with Meniere's disease. Laryngoscope 2007;117:415–20.
[5] Horii A, Osaki Y, Kitahara T, Imai T, Uno A, Nishiike S, et al. Endolymphatic hydrops in Meniere's disease detected by MRI after intratympanic administration of gadolinium: comparison with sudden deafness. Acta Otolaryngol 2011;131:602–9.
[6] Uno A, Imai T, Watanabe Y, Tanaka H, Kitahara T, Horii A, et al. Changes in endolymphatic hydrops after sac surgery examined by Gd-enhanced MRI. Acta Otolaryngol 2013;133:924–9.
[7] Uno A, Horii A, Imai T, Osaki Y, Kamakura T, Kitahara T, et al. Endolymphatic hydrops detected with inner ear gd contrast-enhanced MRI; comparison between administration routes or with ECochG or glycerol test. Nihon Jibiinkoka Gakkai Kaiho 2013;116:960–8.
[8] Friedmann DR, Eubig J, McGill M, Babb JS, Pramanik BK, Lalwani AK. Development of the jugular bulb: a radiologic study. Otol Neurotol 2011;32:1389–95.
[9] Wadin K, Thomander L, Wilbrand H. Effects of a high jugular fossa and jugular bulb diverticulum on the inner ear. A clinical and radiologic investigation. Acta Radiol Diagn 1986;27:629–36.
[10] Jahrsdoerfer RA, Cail WS, Cantrell RW. Endolymphatic duct obstruction from a jugular bulb diverticulum. Ann Otol Rhinol Laryngol 1981;90:619–23.
[11] Miyashita T, Toyama Y, Inamoto R, Mori N. Evaluation of the vestibular aqueduct in Ménière's disease using multiplanar reconstruction images of CT. Auris Nasus Larynx 2012;39:567–71.

Please cite this article in press as: Oya R, et al. A high jugular bulb and poor development of perivestibular aqueductal air cells are not the cause of endolymphatic hydrops in patients with Ménière's disease. Auris Nasus Larynx (2017), http://dx.doi.org/10.1016/j.anl.2017.09.014

[12] Wilbrand HF, Stahle J, Rask-Andersen H. Tomography in Menière's disease—why and how. Morphological, clinical and radiographic aspects. Adv Otorhinolaryngol 1978;24:71–93.
[13] Kennedy DW, el-Sirsy HH, Nager GT. The jugular bulb in otologic surgery: anatomic, clinical, and surgical considerations. Otolaryngol Head Neck Surg 1986;94:6–15.
[14] Okumura T, Imai T, Takimoto Y, Takeda N, Kitahara T, Uno A, et al. Assessment of endolymphatic hydrops and otolith function in patients with Ménière's disease. Eur Arch Otorhinolaryngol 2017;274:1413–21.
[15] Rauch SD, Xu WZ, Nadol Jr JB. High jugular bulb: implications for posterior fossa neurotologic and cranial base surgery. Ann Otol Rhinol Laryngol 1993;102:100–7.
[16] Hourani R, Carey J, Yousem DM. Dehiscence of the jugular bulb and vestibular aqueduct: findings on 200 consecutive temporal bone computed tomography scans. J Comput Assist Tomogr 2005;29:657–62.
[17] Woo CK, Wie CE, Park SH, Kong SK, Lee IW, Goh EK. Radiologic analysis of high jugular bulb by computed tomography. Otol Neurotol 2012;33:1283–7.
[18] Park JJ, Shen A, Keil S, Kuhl C, Westhofen M. Jugular bulb abnormalities in patients with Meniere's disease using high-resolution computed tomography. Eur Arch Otorhinolaryngol 2015;272:1879–84.
[19] Kitahara T, Doi K, Maekawa C, Kizawa K, Horii A, Kubo T, et al. Meniere's attacks occur in the inner ear with excessive vasopressin type-2 receptors. J Neuroendocrinol 2008;20:1295–300.
[20] Maekawa C, Kitahara T, Kizawa K, Okazaki S, Kamakura T, Horii A, et al. Expression and translocation of aquaporin-2 in the endolymphatic sac in patients with Meniere's disease. J Neuroendocrinol 2010;22:1157–64.

Please cite this article in press as: Oya R, et al. A high jugular bulb and poor development of perivestibular aqueductal air cells are not the cause of endolymphatic hydrops in patients with Ménière's disease. Auris Nasus Larynx (2017), http://dx.doi.org/10.1016/j.anl.2017.09.014